Robotica (2001) volume 19, pp. 241–253. Printed in the United Kingdom © 2001 Cambridge University Press

Sagittal gait of a biped robot during the single support phase. Part 2: optimal motion*

Mostafa Rostami and Guy Bessonnet

Laboratoire de Mécanique des Solides – UMR 6610 CNRS, Université de Poitiers, SP2MI, Teleport 2, Bd Marie et Pierre Curie, BP 30179, 86962 Futuroscope Chasseneuil Cedex (France). E-mail: Guy.Bessonnet@lms.univ-poitiers.fr

(Received in Final Form: July 26, 2000)

SUMMARY

The paper is aimed at generating optimal swing motions during the single-support phase of sagittal gait. Unlike the previous Part 1 which deals with passive motions, all joints of the biped are assumed to be active in the present Part 2. The final conditions specify an impactless heel-touch in order to avoid a destabilizing effect on the biped motion. As the biped is essentially submitted to gravity forces, the motion is generated by minimizing the joint actuating torques. Feasible motions are defined by state inequality constraints limiting joint motions, and defining foot clearance and obstacle avoidance during the swing. The optimization problem is dealt with using Pontryagin's Maximum Principle. A final two-point boundary value problem is solved by implementing a shooting method. The approach presented is illustrated by various numerical simulations applying to a seven-body planar biped which has four or five active joints during the swing phase.

KEYWORDS: Sagittal gait; Single support phase; Bipedal robot; Dynamics of walking; Motion optimization; Obstacle avoidance.

1. INTRODUCTION

In the field of biped locomotion, our reference model is human gait. Although the kinematics organization of human walking is quite easy to describe, the underlying dynamics is complex to analyze and even more difficult to simulate. On the other hand, if we want to move a legged-robot, a simple means to define its gait consists in introducing a kinematic model of walk. But, even though such a model would seem to be well organized, it would not ensure the quality of its dynamics, that is to say, a good synchronization together with restrained values of joint actuating torques, as well as moderate energy consumption. This is a major reason to search for an organizing principle of the dynamics of biped locomotion, able to generate reference steps. Such an objective is pursued in many works dealing with gait dynamics with an optimization aspect.

The prevailing idea is based on the minimization of a performance criterion with a dynamic content involving essentially the joint actuating torques, or the energy consumption. An interesting first attempt to generate an optimal step is extensively developed in reference [1]. The problem is stated using a simplified dynamic model of the biped moving in the sagittal plane. The hip trajectory is prescribed during the whole gait cycle, while the ankle trajectory is only specified during the swing phase. Thus, the optimal motion generated comprises only two degrees of freedom, which is quite restrictive. In fact, the main interest of this work is the approach presented to deal with the optimization problem, which is stated within the frame of the optimal control theory. Accordingly, the implemented optimization technique is the Pontryagin Maximum Principle (PMP). Kinematic constraints are taken into account by means of an augmented integral criterion, and are dealt with using a penalty method. In this way, the constrained optimization problem is transformed into a sequence of unconstrained problems which are solved as two-point boundary value problems. We use a similar approach in our paper, but on the basis of a global dynamic model of the biped.

Hatze[2] applies the PMP to generate an optimal dynamic behaviour of a musculo-skeletal model of a human locomotion limb. The performance index is the minimum time required to transfer the mechanical system from a given initial position to a specified final position. The author concludes that another relevant criterion to be minimized would be the total energy expended by muscles during the motion. Still for the case of human gait, Bourassa *et al.*,[3] make a different choice by introducing the minimization of muscular efforts. Three characteristic phases of gait (posture, deployment and swinging) are studied by introducing a set of suitable constraints. The movement of the hip is prescribed, and the trunk motion can be dealt with separately.

Another approach to gait optimization consists in using parameterization techniques.[4–9] Parameterizing a motion means that it is partly defined by means of explicit but incompletely specified time functions. Using this approach, the optimization problem is drastically simplified. In fact, it can be reduced to the minimization of an algebraic function depending on a finite number of discrete unknown variables. The final problem may be solved using different techniques, the prevalent one being sequential quadratic programming. Two different approaches are used to partly specify the biped movement. In references [4, 6] this motion is described in the operational space by representing the hip trajectory together with the ankle trajectory of the swing foot. As in references [5, 7–9] the alternative approach consists in representing directly the joint coordinates. In

* Part 1 appeared in the previous issue of *Robotica* (Vol. 19, Part 2, pp. 163–176).

https://doi.org/10.1017/S0263574700003039 Published online by Cambridge University Press

both cases, the time functions used are polynomials or finite Fourier series. The problem unknowns are simply the coefficients of these functions. In reference [8] a 6-body biped without a trunk is studied, while in other papers, 5-body bipeds are modeled. The performance criterion to be minimized represents an energetic cost as in references [4–8], or the integral quadratic norm of joint actuating torques.[7–9] In most cases, the kinematic model of gait comprises an instantaneous double support phase with impact at heel-touch. In other respects, inequality constraints expressing the unilaterality of contact with the ground are verified *a posteriori*. Parameterization techniques yield sub-optimal solutions.

Another interesting contributing to human gait optimization is found in reference [10]. The authors compare the optimal motions generated by seven different performance criterions. They conclude that the optimizing index which is suited at best to human gait is the minimization of joint actuating torques.

Let us mention that many bipedal walking machines have been designed during the last two decades. The reader is especially referred to references [11–15] describing biped robots that have walked. Suitable control techniques must be developed to produce efficient walk with a moderate dynamic cost. In reference [11], the authors emphasize the fact that a preliminary problem consists in selecting good trajectories. This concern reappears in references [14, 15] where the local controller controls joint actuators in order for the robot to follow preset walking patterns. Thus, generating reference gait patterns in the context of motion control is a relevant means for mastering the biped dynamics, especially for the case when the inertia and mass of the legs are sizeable, and when the biped does not walk at a slow pace.

In the present paper, motions to be generated do not depend on any preliminary kinematic representation. The minimization of an integral cost yields directly an optimal step satisfying constraints which define feasible motions. As in most of papers above mentioned, our study is focused on the swing phase of sagittal gait. We consider a 7-body planar biped with a trunk and anthropomorphic feet. Due to the fact that the biped is essentially submitted to gravity forces, we have favored the minimization of joint actuating torques instead of energy expenditure. Moreover, as Blajer and Schiehlen[16] did for motion control of a biped, we invoke the destabilizing effect of impact at heel-touch to motivate the search for an impactless gait at the end of the single-support phase. Feasible motions are defined by state constraints limiting the joint movements, and preventing foot collision with the ground or an obstacle.

The optimization problem, and particularly the dynamic model of the biped are especially formulated for applying the Pontryagin Maximum Principle. An efficient implementation of this powerful mathematical tool requires to have recourse to Hamiltonian formalism. This formulation is presented in the second section of the paper. In the third section we detail the constraints which define feasible motions. The fourth section is devoted to the formulation of an optimal control problem together with the necessary conditions of optimality stated by the PMP. We present a variety of numerical simulations in the fifth section. We present conclusions in section six, and indicate perspectives for developing the approach presented.

2. KINEMATICS AND DYNAMICS OF A PLANAR BIPED

The planar multibody system which models the biped is similar to the reference model used in the companion paper (Part 1). But, in the present case, more free joints are considered, and all of them are powered. A complete Hamiltonian dynamic model is formulated on the basis of a set of relative joint coordinates.

2.1 Kinematic model

We describe a sagittal model of an anthropomorphic biped. Figure 1 shows the diagram of the biped at initial time (toe-off) and final time (heel-touch) of the swing phase.

This model is made up of 7 limbs numbered from L_0 to L_6. The three first links (L_0 to L_2) represent the foot, the shin and the thigh of the stance leg. The next one L_3 is the trunk, while L_4 to L_6 stand for the thigh, the shin and the foot of the swing leg. Such a planar system comprises six joints: two ankles, two knees and two coaxial hip joints. This model makes it possible to simulate the human gait in the sagittal plane when the sway motion (frontal rotation of the pelvis) is not very important. As we assume that the stance foot remains motionless and flat on the ground during all the swing phase, the biped motion can be described by the six relative joint coordinates we define as:

$$q_i = (X_i, X_{i-1})_{Z_0}, \quad i = 1, \ldots, 6 \quad (Z_0 = X_0 \times Y_0) \quad (1)$$

Let us add the complementary notations

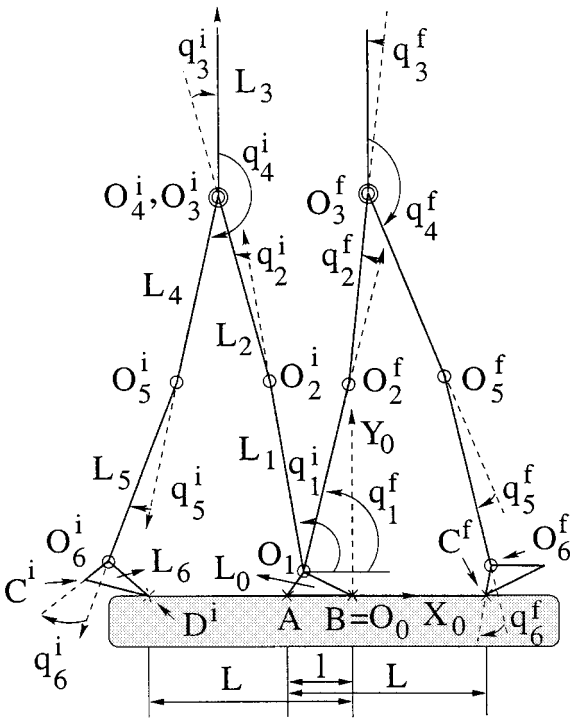

Fig. 1. 7-link planar biped at toe-off and heel-touch.

https://doi.org/10.1017/S0263574700003039 Published online by Cambridge University Press

$\mathbf{q} = (q_1, \ldots, q_6)^T$, vector of joint coordinates
$\dot{\mathbf{q}} = (\dot{q}_1, \ldots, \dot{q}_6)^T$, vector of joint velocities
$\ddot{\mathbf{q}} = (\ddot{q}_1, \ldots, \ddot{q}_6)^T$, vector of joint accelerations

where $\dot{q}_i = dq_i/dt$, $\ddot{q}_i = d^2q_i/dt^2$.

In accordance with the schematic representation in Figure 1, we define the dimension and inertia characteristics of the biped as

O_iO_{i+1} $= r_iX_i$, $i = 1, \ldots, 5$; r_i , length of link L_i
O_iG_i $= a_iX_i$; G_i, center of inertia of link L_i, $i = 1, \ldots, 5$
O_6G_6 $= a_6X_6 + b_6Y_6$, $(Y_6 = Z_0 \wedge X_6)$
m_i , mass of L_i
I_i^{zz} , moment of inertia of L_i with respect to the joint axis $(O_i; Z_0)$

Numerical values of these dimensional parameters are given in the appendix.

In order to master progressively the computational processing of the optimization problem stated in the next section, we will use initially a simplified 4-dof model with $q_2 = cste$ and $q_6 = cste$ (the knee of the stance leg together with the ankle of the swing leg are locked). Afterwards, by means of these first results, we shall be able to deal with models with extended kinematics.

2.2 Dynamic model

As a preliminary remark, let us underline that it may be computationally quite efficient to formulate a dynamic model adapted at best to the chosen optimization technique. As we intend to use the Pontryagin Maximum Principle (or PMP) for solving the dynamic optimization problem stated in what follows, let us recall that the implementation of the PMP requires the formulation of the dynamic model in state space form. As indicated in references [17, 18] the Hamiltonian dynamic model not only best fulfills this requirement but, as well, strengthens the robustness of algorithms used to solve the optimization problem. We present the outlines of the formulation we need.

Firstly, introducing the Langrangian of the mechanical system

$$L(\mathbf{q}, \dot{\mathbf{q}}) = T(\mathbf{q}, \dot{\mathbf{q}}) - V(\mathbf{q}) \tag{2}$$

where V stands for the gravity potential, and T is the kinetic energy defined as

$$T(\mathbf{q}, \dot{\mathbf{q}}) = 1/2\dot{\mathbf{q}}, \dot{\mathbf{q}}^T\mathbf{M}(\mathbf{q})\dot{\mathbf{q}}\,, \tag{3}$$

$\mathbf{M}$ being the $(n \times n)$ mass matrix of the kinematic chain, Lagrange's equations of motion may be derived as

$$\frac{d}{dt}\left(\frac{\partial L}{\partial \dot{q}_i}\right) - \frac{\partial L}{\partial q_i} = Q_i^d + Q_i^a\,,\ i = 1, \ldots, n\,, \tag{4}$$

where Q_i^a (resp. Q_i^d) represents the joint actuating torque (resp. joint dissipative torque) exerted by L_{i-1} on L_i at O_i (cf. Figure 1).

Secondly, defining the conjugate momenta

$$p_i = \frac{\partial L}{\partial \dot{q}_i}\,, \quad i = 1, \ldots, n\,, \tag{5}$$

and the Hamiltonian

$$H(\mathbf{q}, \mathbf{p}) = \mathbf{p}^T\dot{\mathbf{q}} - L(\mathbf{q}, \dot{\mathbf{q}})\,, \text{ with } \mathbf{p} = (p_1, \ldots, p_n)^T \tag{6}$$

Lagrange's equations in (4) may be reformulated in Hamiltonian form

$$\begin{cases} \dot{q}_i = \frac{\partial H}{\partial p_i} \\ \dot{p}_i = -\frac{\partial H}{\partial q_i} + Q_i^a + Q_i^d \end{cases} \tag{7}$$

Now, considering (2) and (3), the expression of $\mathbf{p}$ can be written through (5) as

$$\mathbf{p} = \mathbf{M}\dot{\mathbf{q}}$$

or, inversely

$$\dot{\mathbf{q}} = \mathbf{M}^{-1}\mathbf{p}$$

Using these expressions in (3) and (6), one obtains:

$$H(\mathbf{p}, \mathbf{q}) = \frac{1}{2}\mathbf{p}^T\mathbf{M}^{-1}\mathbf{p} + \mathbf{V}$$

Then, (7) becomes more explicitly

$$\begin{cases} \dot{q}_i = G_i(\mathbf{q}, \mathbf{p}) \equiv \sum_{j=1}^n M_{ij}^{-1}p_j \\ \dot{p}_i = -\frac{1}{2}\mathbf{p}^T\mathbf{M}_{,i}^{-1}\mathbf{p} - \mathbf{V}_{,i} + Q_i^a + Q_i^d \end{cases} \tag{8}$$

where $\mathbf{M}_{,i}^{-1} \equiv \partial\mathbf{M}^{-1}/\partial q_i$, $\mathbf{V}_{,i} \equiv \partial\mathbf{V}/\partial q_i$.

In (8) the presence of the derived matrices $\mathbf{M}_{,i}^{-1}$ makes this formulation impracticable. But, defining the vector $\mathbf{G} = (G_1, \ldots, G_n)^T$ (see (8)) and using the formula $(\mathbf{M}^{-1})_{,i} = -\mathbf{M}^{-1}\mathbf{M}_{,i}\mathbf{M}^{-1}$, the set of equations (8) can be reformulated on the basis of the derived matrices $\mathbf{M}_{,i}$ (instead of $\mathbf{M}_{,i}^{-1}$ in (8)) as

$$\begin{cases} \dot{q}_i = G_i(\mathbf{q}, \mathbf{p}) \\ \dot{p}_i = \frac{1}{2}\mathbf{G}^T\mathbf{M}_{,i}\mathbf{G} - V_{,i} + \mathrm{Q}_i^a + \mathrm{Q}_i^d \end{cases} \tag{9}$$

With this formulation,[17] Hamiltonian equations are ideally structured for applying the Pontryagin Maximum Principle.

Now, defining

$$i \le n \begin{cases} x_i = q_i \\ x_{n+i} = p_i \\ u_i = Q_i^a \end{cases}$$

$\mathbf{x} = (x_1, \ldots, x_{2n})^T$, vector of state variables
$\mathbf{u} = (u_1, \ldots, u_n)^T$, vector of control inputs (joint actuating torques)

$F_i \equiv G_i = \sum_{j=1}^n M_{ij}^{-1}x_{n+j}$

$\mathbf{G} = (G_1, \ldots, G_n)^T$
$F_{n+i} = 1/2\mathbf{G}^T M_{,i}\mathbf{G} - V_{,i} + Q_i^d$
$\mathbf{F} = (F_1, \ldots, F_{2n})^T$,

the double set of vectorial equations (7) can be recast as the 2n-order differential vector-equation:

https://doi.org/10.1017/S0263574700003039 Published online by Cambridge University Press

$$\dot{\mathbf{x}}(t) = \mathbf{F}(\mathbf{x}(t)) + \mathbf{B}\mathbf{u}(t) \equiv \mathcal{F}(\mathbf{x}(t), \mathbf{u}(t)) \tag{10}$$

where **F** is a nonlinear function in **x**, and **B** is the constant $(2n \times n)$ matrix such as

$$\mathbf{B} = \begin{bmatrix} \mathbf{B}_1 \\ \mathbf{B}_2 \end{bmatrix}, \quad \mathbf{B}_1 = \mathbf{0}_{n\times n}, \quad \mathbf{B}_2 = \mathbf{I}_{n\times n} \tag{11}$$

In this equation, initial and final states will be specified as

$$k \le n, \begin{cases} x_k(t^i) = q_k^i, x_k(t^f) = q_k^f \\ \dot{x}_k(t^i) = p_k(t^i) = \sum_{j\le n} M_{kj}(\mathbf{q}^i)\dot{q}_j^i \\ \dot{x}_k(t^f) = p_k(t^f) = \sum_{j\le n} M_{kj}(\mathbf{q}^f)\dot{q}_j^f \end{cases} \tag{12}$$

where it will be assumed in subsection 3 that initial and final Langrangian phase-variables q_k^i, $\dot{q}_k^i$, q_k^f, $\dot{q}_k^f$, have specified values. Consequently, initial and final Hamiltonian states $\mathbf{x}(t^i)$ and $\mathbf{x}(t^f)$ will be entirely specified as well.

Let us mention that a complementary transformation remains to be achieved in order to perfect formulation (9, 10, 12). It consists in rescaling all the variables of the problem to homogenize their order of magnitude. To that end, one can introduce the following reference quantities: $\bar{L}$, $\bar{M}$, $\bar{T}$, $\bar{I}$, $\bar{Q}$, respectively length, mass, time, moment of inertia and torque of reference which can be defined and linked as

$$\begin{aligned} &\bar{M} = \tfrac{1}{n}(m_1 + \ldots + m_n) \\ &\bar{Q} = \tfrac{1}{n}(Q_1^{a,max} + \ldots + Q_n^{a,max}) \\ &\bar{I} = \bar{M}\bar{L}^2, \ \bar{T} = \sqrt{\frac{\bar{I}}{\bar{Q}}} \end{aligned} \tag{13}$$

where m_i is the mass of link L_i, and $Q_i^{a,max}$ is the maximal value of $|Q_i^a|$.

Also, let τ be the reduced time $\tau = \frac{t}{\bar{T}}$. Then, we define adimensional state variables x_j as

$$i \le n, \begin{cases} x_i(\tau) = q_i(t) \\ x_{n+i}(\tau) = p_i(t)/\bar{M}\,\bar{L}^2\,\bar{T}^{-1} \end{cases}, \tag{14}$$

together with normalized actuating torques

$$u_i(\tau) = Q_i^a(t)/Q_i^{a,max} \equiv Q_i^a(t)/\nu_i\bar{Q}, \tag{15}$$

where ν_i stands for the adimensional coefficient $\nu_i = Q_i^{a,max}/\bar{Q}$.

With these new variables, equation (10) remains formally unchanged, except that the matrix $\mathbf{B}_2$ becomes $\mathbf{B}_2 = diag(\nu_1, \ldots, \nu_n)$.

3. FEASIBLE MOTIONS AND CONSTRAINTS

Feasible motions of the biped are defined by two types of specific conditions: The first type consists of state constraints involving the phase coordinates $\mathbf{q}_i$, $\dot{\mathbf{q}}_i$ $(i \le n)$ through the state variables x_j $(j \le 2n)$. The second type specifies interaction conditions between the stance foot and the ground.

3.1 State constraints

Such constraints may be instantaneous when considering conditions imposed at toe-off and heel-touch, or permanent when they must be fulfilled during the whole interval of time.

3.1.1 Initial and final constraints. As in the companion paper these constraints specify the conditions of toeing-off and heel-touch at start and end of the swing motion.

Initial conditions are primarily formulated as vectorial projections

$$\begin{aligned} &OD^i \cdot X_0 + L = 0, \\ &OD^i \cdot Y_0 = 0, \\ &V(D^i) \cdot X_0 = 0, \\ &V(D^i) \cdot Y_0 = 0, \end{aligned} \tag{16}$$

the two first relationships indicating that the foot tip is in contact with the ground at the right place, the two next ones expressing that the same point C^i (Figure 1) has no initial velocity at the beginning of the swing motion. But, on the other hand, the foot may have a rotation velocity about the point C^i at the initial time.

We formulate quite similar conditions at final time

$$\begin{aligned} &OC^f \cdot X_0 - (L - l) = 0, \\ &OC^f \cdot Y_0 = 0, \\ &V(C^f) \cdot X_0 = 0, \\ &V(C^f) \cdot Y_0 = 0, \end{aligned} \tag{17}$$

the two first ones expressing a symmetrical repositioning of the swing foot on flat ground (l stands for the foot length as indicated in Figure 1). The last two prescribe an impactless heel-touch. This is the main difference between conditions (17) and similar conditions formulated in Part 1 of the paper; in what follows, zero impact velocity will be exactly satisfied by any optimal solution while in the previous study we only tried to reduce the velocity of point C^f at heel-touch.

Constraints (16, 17) can be formally expressed as

$$k \le 4, \begin{cases} C_k^i(\mathbf{q}^i, \dot{\mathbf{q}}^i) = 0 \\ C_k^f(\mathbf{q}^f, \dot{\mathbf{q}}^f) = 0 \end{cases} \tag{18}$$

As in reference [19], at both initial and final times we specify the position of the trunk and assume that its absolute rotation rate is equal to zero, which implies a relationship

$$\begin{aligned} &\sum_{k\le 3} q_k^i = \sum_{k\le 3} q_k^f = \alpha \\ &\sum_{k\le 3} \dot{q}_k^i = \sum_{k\le 3} \dot{q}_k^f = 0 \end{aligned} \tag{19}$$

where the value of α is either equal or close to $\pi/2$.

We define, as well, the joint coordinates and velocities of the stance leg:

$$k = 1, 2, \begin{cases} q_k(t^i) = q_k^i, \ \dot{q}_k(t^i) = \dot{q}_k^i \\ q_k(t^f) = q_k^f, \ \dot{q}_k(t^f) = \dot{q}_k^f \end{cases} \tag{20}$$

where q_k^i and q_k^f are given, while $\dot{q}_k^i$ and $\dot{q}_k^f$ are chosen in order to respect a given mean-value of the hip velocity.

https://doi.org/10.1017/S0263574700003039 Published online by Cambridge University Press

Lastly, we specify the ankle coordinates and velocities of the swing foot:

$$\begin{aligned} q_6(t^i) &= q_6^i \quad , \quad \dot{q}_6(t^i) = \dot{q}_6^i \\ q_6(t^f) &= q_6^f \quad , \quad \dot{q}_6(t^f) = \dot{q}_6^f \end{aligned} \tag{21}$$

where quantities in right hand members represent given values.

Then, taking into account data (19), (20) and (21), the constraints (18) may be solved in order to completely define initial and final conditions, namely, $\mathbf{q}^i$, $\dot{\mathbf{q}}^i$, $\mathbf{q}^f$, $\dot{\mathbf{q}}^f$.

3.1.2 Bound constraints. In order to respect joint stops, to prevent counter-flexion and to moderate total joint coordinate variations, we must prescribe bounds on joint coordinates, defined as the box constraints

$$t \in [t^i, t^f],\ i \le n,\ q_i^{min} \le q_i(t) \le q_i^{max} \tag{22}$$

where q_i^{min} and q_i^{max} are specified values.

This set of double inequalities can be recast under the standard form of $2n$ simple constraints

$$\begin{cases} h_i(\mathbf{q}(t)) \le 0 \quad , \quad \text{where} \quad h_i(\mathbf{q}(t)) = q_i(t) - q_i{}^{max} \\ h_{n+1}(\mathbf{q}(t)) \le 0 \quad , \quad \text{where} \quad h_{n+i}(\mathbf{q}(t)) = q_i{}^{min} - q_i(t) \end{cases} \tag{23}$$

In fact, the only useful constraints we need in our problem concern both knee and ankle coordinates of the swing leg. Other joint coordinates will keep spontaneously appropriate values.

3.1.3. Foot clearance. During the swing phase, intermediate contact of the foot with the ground must be prevented. The biped should be able as well to step over low-sized obstacles. In a general way, biped abilities to clear an obstacle, to step across a sill and to climb stairs, are many advantageous intrinsic features of bipedal locomotion.

A simple means to model obstacle avoidance by the swing foot in the sagittal plane consists in defining a collision zone surrounding the obstacle. As indicated in Figure 2, the upper boundary of this area may be represented by a curve which can be defined by a simple function. For instance, the 5th degree polynomial

$$\varphi(x) = a_0 + a_1(x-d) + a_2(x-d)^2 + \ldots + a_5(x-d)^5 \tag{24}$$

may be adjusted so as to go through the points D', E and C' with a null slope at these points (Figure. 2). Both points D' and C' could also coincide with D^i and C^f respectively.

The coefficient $a_0, \ldots, a_5$ must be computed with respect to the values of parameters c, l and h (see Figure 2) which are positive constants.

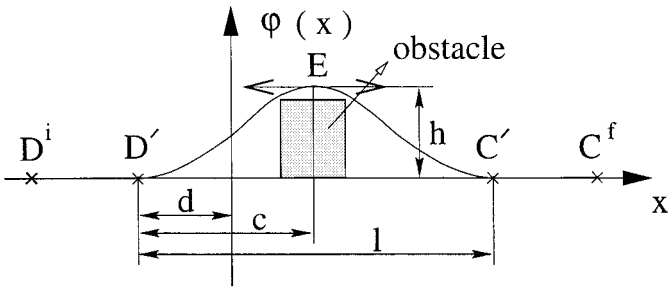

Fig. 2. Collisional zone surrounding an obstacle

It is obvious that $a_0 = a_1 = 0$. Other coefficient can be expressed using the formula

$$[a_2\ a_3\ a_4\ a_5]^T = \mathbf{B}^{-1}[0\ 0\ h\ 0]^T$$

where

$$\mathbf{B} = \begin{pmatrix} 2l & 3l^2 & 4l^3 & 5l^4 \\ l^2 & l^3 & l^4 & l^5 \\ c^2 & c^3 & c^4 & c^5 \\ 2c & 3c^2 & 4c^3 & 5c^4 \end{pmatrix}$$

In Figure 3, the swing foot passes through a collision zone.

Since the variation of the rotation angle of the foot at ankle is limited, one can say that the foot avoids the obstacle if any point of the sole $C\,D$ (Figure 4) remains outside the upper boundary of the collision zone. This condition is expressed as

$$\forall t \in [0, T],\ \forall P \in CD,\ h_P(\mathbf{q}(t)) \equiv \varphi(x_P(\mathbf{q}(t)) - y_P(\mathbf{q}(t)) \le 0$$

where the function φ defines the curve surrounding the obstacle.

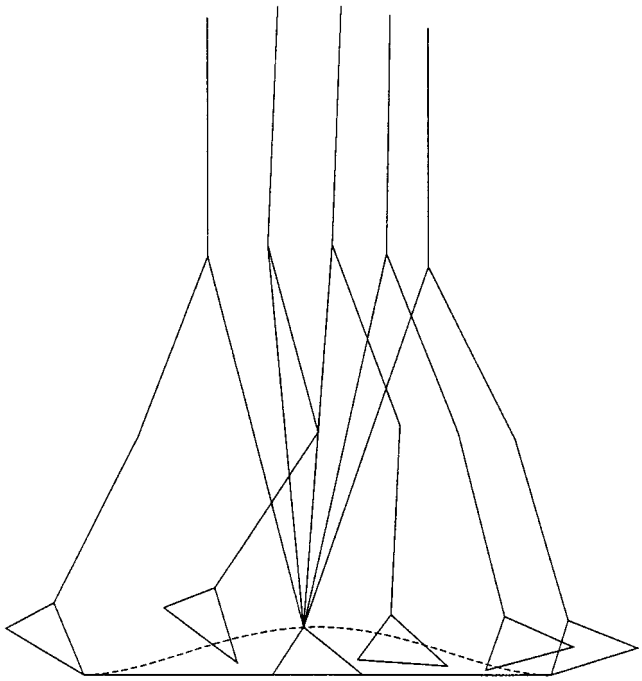

Fig. 3. Foot going through a collisional zone.

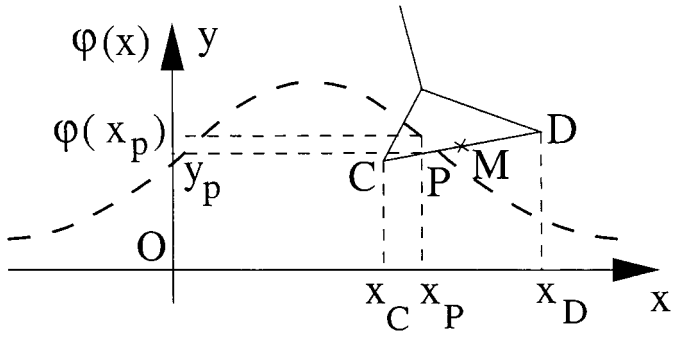

Fig. 4. Collisional zone delimited by the ground and the dotted curve.

https://doi.org/10.1017/S0263574700003039 Published online by Cambridge University Press

In fact, as we expect that the foot motion is smooth, a limited number of points belonging to the segment *C D* can be sufficient to ensure foot clearance. In practice, both end points *C*, *D* and the middle point *M* are enough to produce obstacle avoidance.

In this way, the conditions to satisfy are:

$$\forall t \in [0, T] \ , \begin{cases} h_C(\mathbf{q}(t)) \equiv \varphi(x_C(\mathbf{q}(t))) - y_C(\mathbf{q}(t)) \le 0 \\ h_D(\mathbf{q}(t)) \equiv \varphi(x_D(\mathbf{q}(t))) - y_D(\mathbf{q}(t)) \le 0 \\ h_M(\mathbf{q}(y)) \equiv \varphi(x_M(\mathbf{q}(t))) - y_M(\mathbf{q}(t)) \le 0 \end{cases} \quad (25)$$

3.2 Sthenic constraints

In contrast with state or kinematic constraints, we term *sthenic constraints* the inequalities defining limitations on some forces and torques acting on the mechanical system.

3.2.1. Box constraints. Torques produced by actuators have limited values. When they are considered at the joint level, with the notations introduced in subsection 2.2, we can write

$$\forall t \in [0, T] \ , \quad |Q_i^a(t)| \le Q_i^{a,\,max}$$

These box constraints allow the set of feasible normalized control-variables u_i shown in (15), to be defined as

$$\mathcal{U} = \{(u_1, \ldots, u_i, \ldots, u_n) \in \Re^n / u_i \in [-1, 1], i \le n\} \quad (26)$$

which is a centered parallelepiped in $\Re^n$.

3.2.2. Unilaterality of contact. In the presented models, we assume that the foot of the stance leg stays motionless throughout the movement.

The unilaterality of contact is expressed by the fact that the vertical component of the ground reaction forces must remain positive during the motion. This condition simply means that the foot is not stuck on the ground and that the ground cannot pull but only push the foot.

In order to easily implement this condition, we consider that the ground reaction forces can be equivalently represented by two normal forces N_A and N_B applied at end points *A* and *B* of the foot (see Figure 5), together with a horizontal force acting on the sole. The latter will not be taken into consideration in our present problem. This means the friction coefficient between the sole and the ground is assumed to have a sufficiently great value to prevent any sliding of the stance foot.

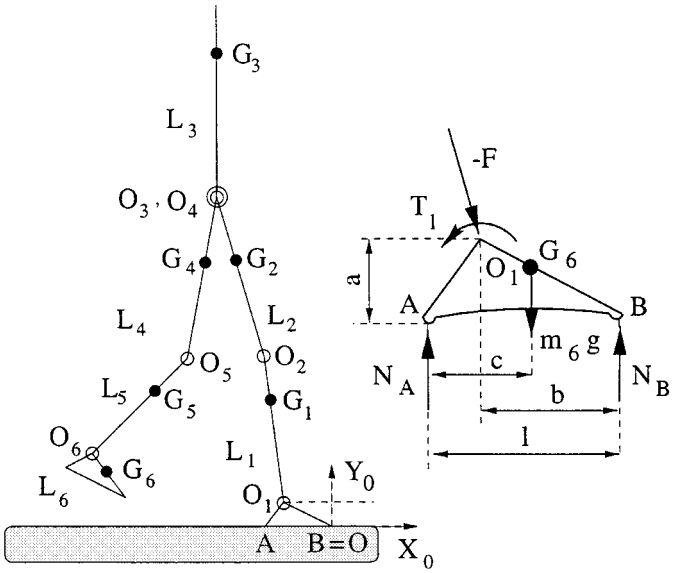

Fig. 5. Forces applied on the stance foot.

Noting:

— F, the total force exerted by the ground on the foot,
— T_1, the torque exerted about O_1 by the foot on the shin,

one obtains the relationships:

$$\begin{aligned} N_B &= \tfrac{1}{l}(T_1 - F_Y(l-b) - aF_X + cm_6 g) \\ N_A &= m_6 g - F_Y - N_B \end{aligned} \quad (27)$$

where F_X and F_Y stand for the component of F with respect to X_0 and Y_0 (see Figure 5).

Expressions of these components are found by formulating Newton's equation of motion for the whole biped, which yields

$$\begin{aligned} F_X &= -\textstyle\sum_{i=1}^{6} m_i \vec{\gamma}(G_i) \cdot \vec{X}_0 \\ F_Y &= -\textstyle\sum_{i=1}^{6} m_i \vec{\gamma}(G_i) \cdot \vec{Y}_0 - \sum_{i=1}^{6} m_i g \end{aligned} \quad (28)$$

With these expressions for F_X and F_Y in (27), the unilaterality conditions are expressed as

$$N_A > 0 \ , \quad N_B > 0 \quad (29)$$

In the following, the fulfillment of constraints (29) will be realized by weakening the stance ankle torque in the optimization process.

4. FORMULATING AN OPTIMAL CONTROL PROBLEM

We wish to generate an optimal swing transfer by minimizing a performance criterion representing a dynamic cost. Roughly speaking, we have the choice between minimizing actuating torques as in references [19, 20], or energy expenditure.[21,22] Since the biped stands and moves in a vertical plane, it is essentially submitted to gravity. For this reason, we have favored the first choice by introducing the integral cost

$$J(\mathbf{u}) = \int_{t^i}^{t^f} L(\mathbf{x}(t), \mathbf{u}(t))dt \quad (30)$$

where the Langrangian is the quadratic function of the normalized control-variables u_i

$$L(\mathbf{x}, \mathbf{u}) \equiv \tfrac{1}{2} \textstyle\sum_{i=1}^{n} \xi_i \nu_i^2 u_i^2 \quad (31)$$

where ξ_i's are weighting factors and $\nu_i u_i$'s represent adimensional joint actuating torques as defined by (15).

Let us mention that criteria like (30, 31) have been implemented to optimize the motions of vertical serial manipulatory arms in references [18, 23]. But, we shall use this cost in a somewhat different way due to the fact that the weighting coefficent can play a much more useful role in the problem we are stating. At first, let us point out that when ξ_i increases, the optimal corresponding u_i is lowered. We will make use of this possibility to reduce the action of both ankle torques in order, firstly, to avoid an optimal motion of

https://doi.org/10.1017/S0263574700003039 Published online by Cambridge University Press

the swing foot with a too large amplitude, and secondly, to fulfill indirectly the unilateral constraints (29).

4.1 Dealing with the state inequality constraints

Such constraints defined in subsection 3.1 can be easily dealt with using computing techniques similar to the penalty method developed in the frame of mathematical programming.[24] We have chosen to implement an exact penalty method defined by introducing the positive functions

$$i \le N_h \ , \ h_i^+(\mathbf{x}(t)) = \max(0, h_i(\mathbf{x}(t)) + b_i) \ , \ b_i \ge 0$$

where each positive constant b_i defines an augmented constraint. This penalty technique consists in minimizing h_i^+ functions when the constraint is infringed, in order to bring h_i functions back to zero. This operation is carried out by minimizing the augmented criterion

$$J_r(\mathbf{u}) = J(\mathbf{u}) + \tfrac{r}{2}\int_{t^i}^{t^f} \mathbf{h}^+(\mathbf{x}(t))^T \mathbf{D_h} \mathbf{h}^+(\mathbf{x}(t)) dt \ , \ r > 0 \quad (32)$$

where $\mathbf{h}^+ = (h_1^+, \ldots, h_{N_h}^+)^T$, and $\mathbf{D_h} = \mathrm{diag}(\zeta_1, \ldots, \zeta_{N_h})$ is a weighting matrix.

The functional J_r must be minimized with sufficiently great value of the penalty multiplier r. But, for increasing values of r the numerical conditioning of the optimization problem deteriorates. A simple means to avoid a too great value of r consists in choosing not too small values for the b_i's.

4.2 Applying Pontryagin's Maximum Principle

At this point, the minimization problem may be summarized as: find a phase trajectory $t \rightarrow \mathbf{x}(t)$, and a control vector $t \rightarrow \mathbf{u}(t)$ minimizing J_r, namely

$$\begin{array}{l} \min \ J_r(\mathbf{u}), \\ \mathbf{u} \in \mathcal{U} \\ r \ \text{great} \end{array} \quad (33)$$

and satisfying the state equation

$$t \in [t^i, t^f] \ , \ \dot{\mathbf{x}}(t) = F(\mathbf{x}(t)) + \mathbf{B}\mathbf{u}(t) \quad (34)$$

together with the end conditions

$$\mathbf{x}(t^i) = \mathbf{x}^i \ , \ \mathbf{x}(t^f) = \mathbf{x}^f \quad (35)$$

where, in (34), $\mathbf{x}(t) \in \Re^{2n}$, and $\mathbf{u}(t) \in \Re^n$.

Defining the Pontryagin function

$$\mathbf{w} \in \Re^{2n} \ , \ \mathcal{H}(\mathbf{x}, \mathbf{u}, \mathbf{w}) = \mathbf{w}^T(F(\mathbf{x}) + \mathbf{B}\mathbf{u}) - L(\mathbf{x}, \mathbf{u}) \ , \quad (36)$$

the maximum principle[25] states that if $t \rightarrow (\mathbf{x}(t), \mathbf{u}(t))$ is a solution of (33–35), then there exists a costate function $t \rightarrow \mathbf{w}(t)$, $\mathbf{w}(t) \in \Re^{2n}$, satisfying the costate equation

$$\dot{\mathbf{w}}(t)^T = -\partial \mathcal{H} / \partial \mathbf{x} \ , \quad (37)$$

and the maximality condition

$$\mathcal{H}(\mathbf{x}(t), \mathbf{u}(t), \mathbf{w}(t)) = \max_{\mathbf{v} \in \mathcal{U}} \mathcal{H}(\mathbf{x}(t), \mathbf{v}, \mathbf{w}(t)) \quad (38)$$

A prominent interest of the PMP lies in condition (38) which allows the constraints on **u** to be exactly satisfied, and yields through (31), (34) and (36) an explicit expression of the optimal control under the form of the saturation function[25]

$$i \le n \ , \ u_i(t) = \mathrm{Sat}\left[\frac{w_{n+i}(t)}{\xi_i \nu_i}\right] \ , \quad (39)$$

defined here, as

$$\mathrm{Sat}(x) = \begin{cases} x & \text{if} \quad |x| \le 1 \\ x^{max}\ \mathrm{sign}(x) & \text{if} \quad |x| > 1 \end{cases}$$

Substituting the expression (39) for **u** in (34), (37), the unknown functions **x** and **w** appear as a solution of a 4n-order differential system of the type

$$t \in [t^i, t^f] \ , \ \begin{cases} \dot{\mathbf{x}}(t) = \mathcal{F}_1(\mathbf{x}(t), \mathbf{w}(t)) \\ \dot{\mathbf{w}}(t) = \mathcal{F}_2(\mathbf{x}(t), \mathbf{w}(t)) \end{cases} \quad (40)$$

Accompanied by the boundary conditions (35).

Typically, we are in the presence of a two-point boundary value problem.

5. NUMERICAL SIMULATIONS

The two-point boundary value problem (40, 35) can be solved using computing techniques such as finite difference algorithms or shooting methods. We have chosen the latter approach for its efficiency, and the simplicity of its implementation. The technique we use is described in reference [26] as the so-called transition matrix method. Due to the strong non-linearity of equations (40), the main difficulty to overcome in order for the algorithm to converge towards an optimal solution, consists in finding a sufficiently accurate guess solution. This preliminary problem has been dealt with by solving directly the two-point boundary value problem when considering a very short walk-step: about ten centimeters. Then, the optimization problem can be solved iteratively for increasing boundary values, until the desired final values are reached. In the same way, any optimal solution can be used as a guess solution to solve swiftly a problem related to the previous one.

The biped data is given in the appendix. A detailed description of the biped technical characteristics can be found in references [27, 28].

5.1 Optimal motions of a 4-dof biped

We assume that the knee of the stance leg and the ankle of the swing leg are locked during the single support phase. Let us mention that gait with stiff stance leg corresponds to comfortable human walking during which the ankle rotation of the swing foot is quite small.

Thus, in accordance with Figure 1, we have

$$q_2 = 0 \ , \ q_6 = \beta$$

where β is a given constant value. Other joint coordinates are free. Therefore, we must define the following initial and final values of phase coordinates

$$q_j^i, \ \dot{q}_j^i, \ q_j^f, \ \dot{q}_j^f, \ \text{for} \ j = 1, 3, 4, 5$$

which have to satisfy the twelve relationships (18) and (19).

We have chosen q_1^i, $\dot{q}_1^i$, q_1^f, $\dot{q}_1^f$, as given independent values which must be fixed in a coherent way.

https://doi.org/10.1017/S0263574700003039 Published online by Cambridge University Press

Table I. Characteristic data of the swing motion.

$\dot{q}_1^i$ rad/s	$\dot{q}_1^f$ rad/s	L m	T s	$\bar{v}$ km/h	$P\%$
− 1.5	− 1.5	0.51	0.34	3.97	73

Let us add that additional data is the motion time T together with the step length L. A mean walk-speed noted $\bar{v}$ results from the above choices.

For each simulated motion, we present the chosen numerical values of $\dot{q}_1^i$, $\dot{q}_1^f$, L, T, $\bar{v}$ and $P\%$ which represents the percentage of the Single Support Phase (SSP) versus the whole step.

Energy expenditure is computed using the formula

$$E = \int_{t^i}^{t^f} \sum_{i=1}^{n} | \dot{q}_i(t) Q_i^a(t) | \, dt$$

5.1.1 Step lengthening effect. The swing time T being fixed, we compare two optimal motions computed with different step lengths.

Example 1.
The basic data is the step length equal to 0.51 m. Other characteristic values of the swing motion are given in Table I.

The optimal motion which is shown in Figure 6 is quite like human gait. Its average speed is equal to 1.1 m/s (i.e. about 4 km/h). The energy expenditure amounts to 70.6 J. We can compare with the result given in reference [6] which amounts to 75 J for the same speed of gait. But the biped mass in the latter case is equal to 31 kg versus 87 kg in the present paper.

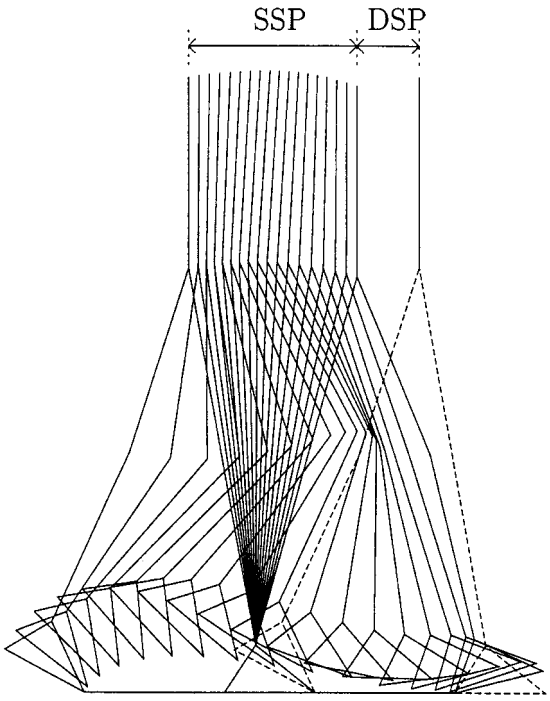

Fig. 6. Optimal gait for a step length equal to 0.51 m. Energy consumption: $E = 70.6$ (J).

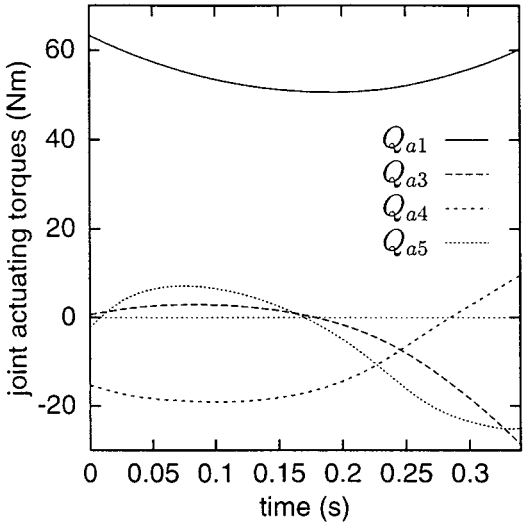

Fig. 7. Gait at moderate speed. Time variations of actuating torques.

The Figures 7 and 8 show the variations of actuating torques and normal ground reaction forces on the stance foot. One can notice that the actuating torque at ankle of the stance leg is positive, i.e. it tends to slow down the motion in order to ensure heel-touch without impact, as specified by the final conditions (17). The normal reaction forces remain positive throughout the motion.

Example 2.
The step length is increased while the transfer time remains unchanged (see Table II). The average gait speed is equal to 1.44 m/s (about 5.2 km/h) versus 1.1 m/s in the previous example.

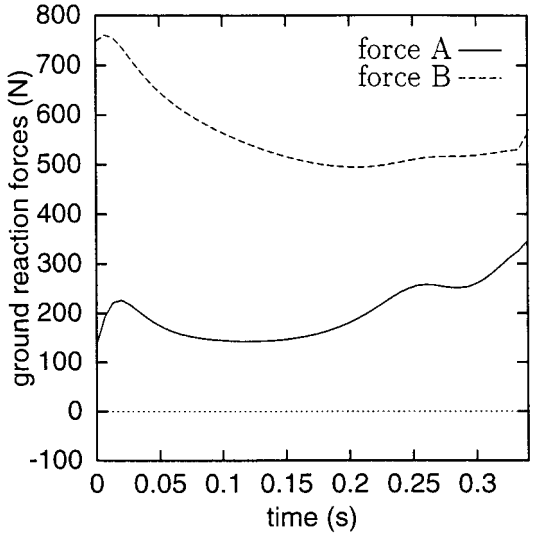

Fig. 8. Normal reaction forces.

Table II. Motion characteristics.

$\dot{q}_1^i$ rad/s	$\dot{q}_1^f$ rad/s	L m	T s	$\bar{v}$ km/h	$P\%$
− 1.95	− 1.95	0.62	0.34	5.2	79

https://doi.org/10.1017/S0263574700003039 Published online by Cambridge University Press

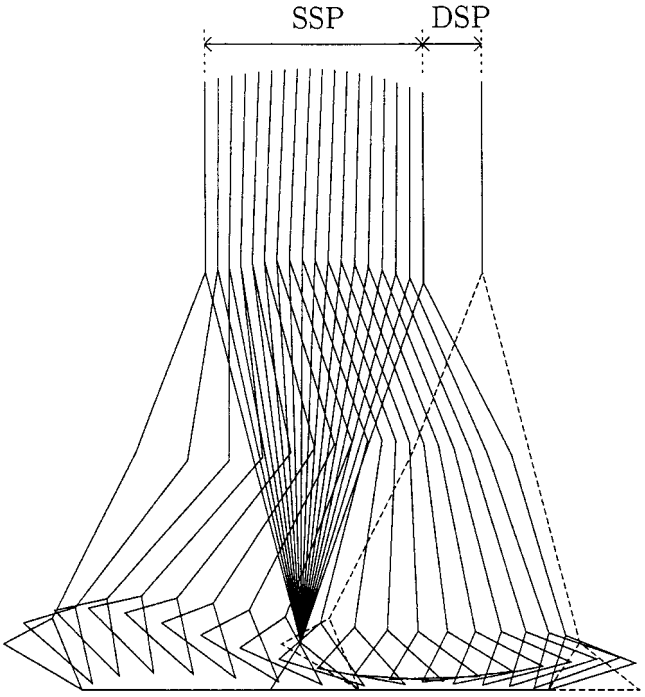

Fig. 9. Fast optimal gait with a step length equal to 0.62 m. Energy consumption: $E = 121.5\ J$.

The optimal motion shown in Figure 9 looks like the previous one, but the heel impact is avoided at the expense of great efforts developed at hip and knee of the swing leg just before the final time (Figures 10 and 11). The energy consumption is greatly increased.

5.1.2 Obstacle avoidance and ground clearance. As one can see in Figure 9, the swing foot only just clears the ground. We want to examine the ability of our approach to generate an optimal motion during which the swing foot gets over an obstacle on the ground. As indicated in subsection 3.1 we use a 5th degree polynomial function φ to define an anti-collision zone which surmounts the obstacle. We impose two null minima at points D^i and C^f, and a maximum height $h = 0.1\ m$ just above the middle point of the segment D^iC^f (see Figures 1 and 12). The coefficients of the function φ, as defined in (24), are determined using the following relations

$$\varphi(x(D^i)) = 0\,, \qquad \dot{\varphi}(x(D^i)) = 0\,,$$
$$\varphi(x(C^f)) = 0\,, \qquad \dot{\varphi}(x(C^f)) = 0\,,$$
$$\varphi(\tfrac{x(D^i)+x(C^f)}{2}) = 0.1\,, \qquad \dot{\varphi}(\tfrac{x(D^i)+x(C^f)}{2}) = 0\,.$$

Other basic characteristics of the step are the same as in the previous example. They are given in Table II.

Figure 12 shows that the collision zone is perfectly avoided by the swing foot. The gait pattern is not quite different of the previous one. But the energy consumption is noticeably increased (140 J versus 121 J).

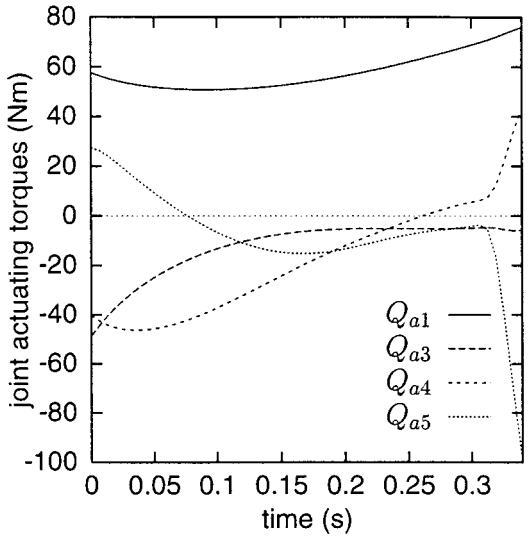

Fig. 10. Fast gait without impact. Time variations of actuating torques.

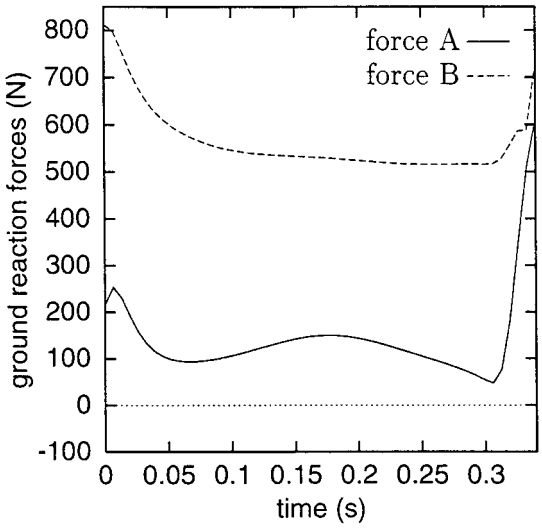

Fig. 11. Normal reaction forces.

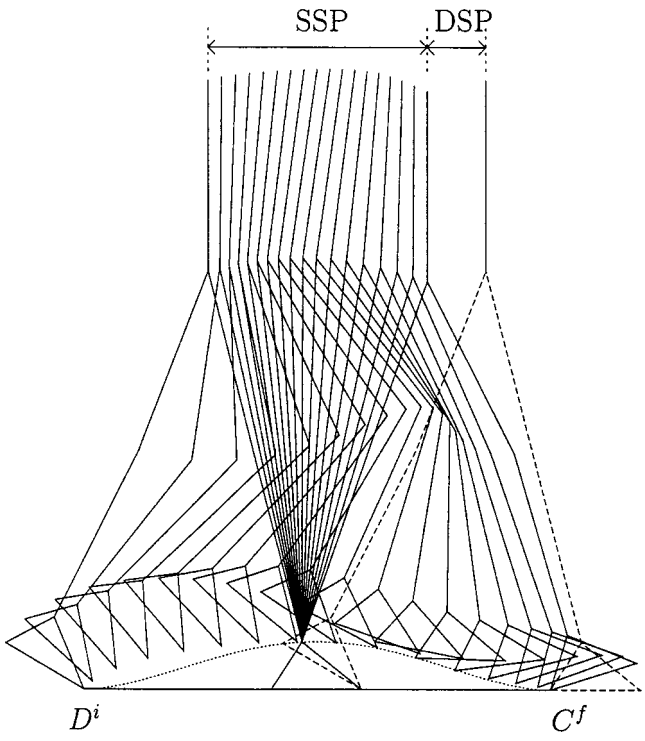

Fig. 12. Stepping over an obstacle.

https://doi.org/10.1017/S0263574700003039 Published online by Cambridge University Press

Table III. Basic data of the motion

$\dot{q}_1^i$ rad/s	$\dot{q}_1^f$ rad/s	L m	T s	$\bar{v}$ km/h	$P\%$
−1.2	−1.13	0.41	0.34	2.9	67

5.1.3 The "heel up" case. As presented in the companion paper, there are two possible configurations initiating the swing phase: the configuration "heel down" and the configuration "heel up". All the results presented in Part 1 of the paper have been computed on the basis of "heel down" initial positions. We present here an optimal motion starting with a "heel up" position of the swing foot. In this case, as shown in Part 1 of the paper, the knee has an initial velocity directed in the opposite direction of gait. This reversed velocity may produce a counter-flexion of the swing leg at the beginning of the swing phase. Then, the introduction of bound constraints as (18), (19) at the knee level is required to avoid hyper-extension.

Moreover, the respect of unilaterality conditions of contact makes necessary to weaken significantly the ankle torque of the stance leg. This can be done by introducing a sufficiently great value of the weighting factor ξ_1 in formula (31) in order that the corresponding normalized torque u_1 becomes weaker as indicated in section 4.

Computing an optimal motion respecting the previous constraints is tricky to carry out. The computation was successful with the data given in Table III.

The optimal motion which appears in Figure 13 shows a gait pattern quite different from the previous examples. The swing foot moves simultaneously backwards and upwards at the beginning of motion. The upward motion is greatly accentuated. The stance leg is nearly immobilized at mid-transfer while the trunk gesticulates significantly. The energy consumption is drastically increased in comparison with the first examples.

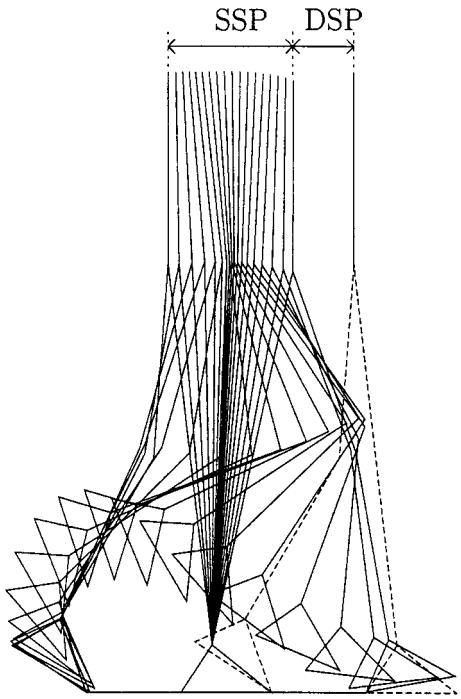

Fig. 13. Movement of the biped. Energy consumption: $E = 249\ J$.

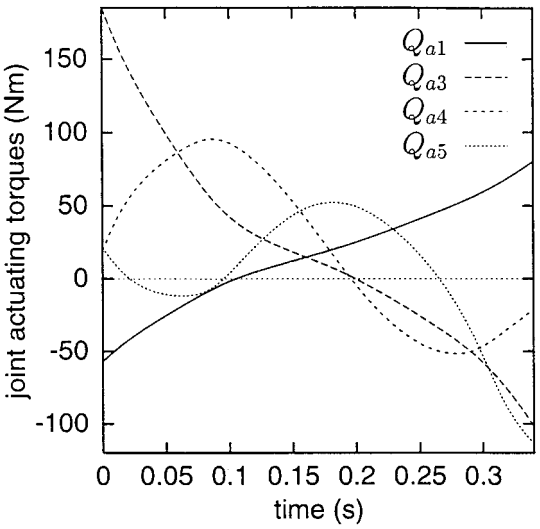

Fig. 14. Time variations of actuating torques.

Figures 14 and 15 show that the ankle actuating torque of the stance leg takes reduced values while the ground reaction forces remain positive during the whole movement. All the constraints are effectively respected, but the motion does not correspond to a natural gait, and is very energy-consuming.

This result brings out the difficulty in generating a feasible motion in case of forward flexion of the leg when there is no ankle at stake. For such locomotion limb with only two joints at hip and knee, an initial backward flexion will help to produce a suitable swing motion. But, in this case, a foot with an appropriate length is required in order to achieve a proper repositioning at heel-touch.

5.2 Optimal motions of a 5-dof biped

We present two examples: In the first one, the stance leg is stiff and the ankle joint of the swing leg is active. Conversely, in the second one, the biped has a flexed stance leg and its ankle joint is locked.

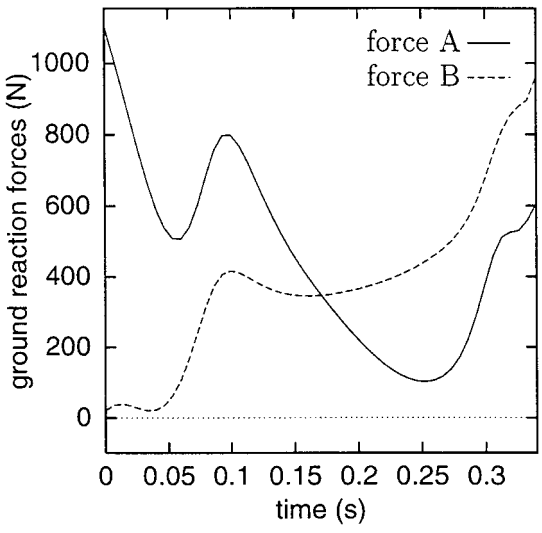

Fig. 15. Normal reaction forces applied to the stance foot.

https://doi.org/10.1017/S0263574700003039 Published online by Cambridge University Press

Table IV. Basic data of the motion

$\dot{q}_1^i$ rad/s	$\dot{q}_1^f$ rad/s	L m	T s	$\bar{v}$ km/h	$P\%$
−1.58	−1.62	0.5	0.33	4.42	81

5.2.1 Actuating the ankle of the swing leg. Both examples have the same step length equal to 0.5 m (see Tables IV and V).

The optimal motion is shown in Figure 16. The rotation of the foot is noticeably marked. In Figure 18 we can see that the evolution of reaction forces indicates a transfer of the weight from heel to forefoot. This forward shift of the weight is paid by a strongly increasing actuating-torque at the ankle of the swing leg (Figure 17). This variation can be interpreted as necessary to ensure the impactless heel-touch which is specified at final time.

5.2.2 Flexing the stance leg. In this case, we specify the following initial and final conditions concerning the knee of the stance leg

$$q_2^i = 10\ (deg)\ , \quad q^f_2 = 1\ (deg)\ ,$$
$$\dot{q}_2^i = 0\ (rad/s)\ , \quad \dot{q}^f_2 = 0\ (rad/s)\ .$$

Table V. Basic data of the motion

$\dot{q}_1^i$ rad/s	$\dot{q}_1^f$ rad/s	L m	T s	$\bar{v}$ km/h	$P\%$
−1.6	−1.6	0.5	0.32	4.33	77

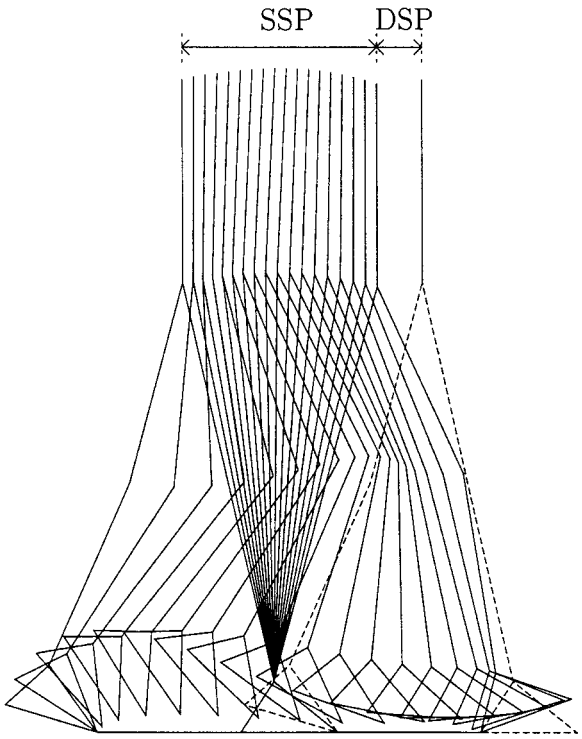

Fig. 16. Optimal motion with actuated ankle at the swing leg. Energy consumption: $E = 75\ J$.

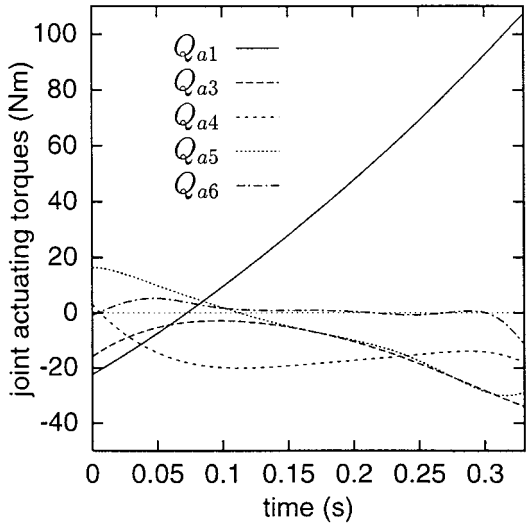

Fig. 17. Joint actuating torques evolution.

Typical features of the motion, given in Table V, are similar to data of Table IV.

The kinematics pattern of the optimal motion shown in Figure 19 is fairly like the previous one.

But the motion dynamics is quite different as one can see in Figures 20 and 21. In fact, the weight transfer does not occur, and simultaneously the actuating torque at ankle of the stance leg keeps positive moderate values. Two different dynamic strategies appear in both optimal motions, and finally, ensure the same impactless condition at heel-touch.

This dissimilarity between dynamics of both motions is mainly due to small differences between initial and final conditions. The result is that the choice of these conditions has great consequences on the way the motion is organized and regulated. This choice should be optimized. This is a perspective in continuing research in the field of optimal gait.

6. CONCLUSION

The kinematics models we have studied gave us an insight into the way bipeds can organize and control their motions during the swing phase.

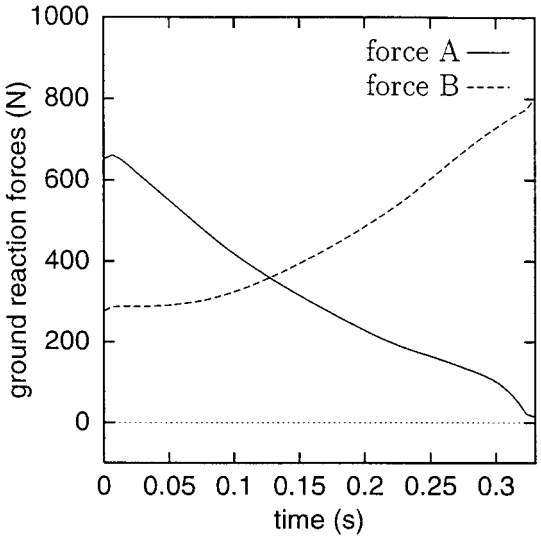

Fig. 18. Normal reaction forces.

https://doi.org/10.1017/S0263574700003039 Published online by Cambridge University Press

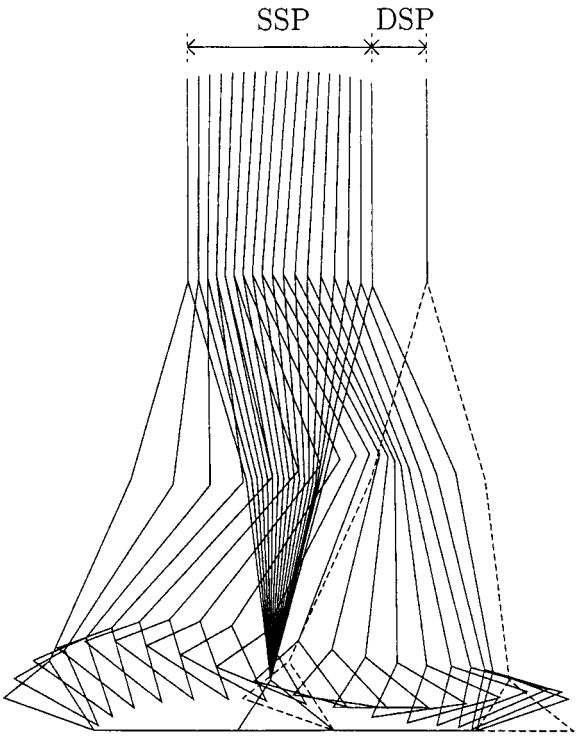

Fig. 19. Optimal movement obtained with flexed stance leg, and for a step length L = 0.5 m. Energy consumption: E 74 J.

We examined the optimal swing motions of a 4-dof biped. In this case, initial forward and backward flexions of the swing leg produce quite different kinematic and dynamic characteristics of optimal motions. Initial forward flexion, corresponding to a "heel-up" position if the shin comprises a foot, does not allow the biped to generate an adequate swing. The motion does not appear natural and its dynamics is not efficient. On the contrary, when the initial flexion is directed backwards, the propelling effect is appropriate, the motion is like a human gait, and the energy expenditure is moderate.

Secondly, we released the ankle joint of the swing foot. In that case, the optimal motion seems quite natural. In the same way, the flexion of the stance leg enables the biped to

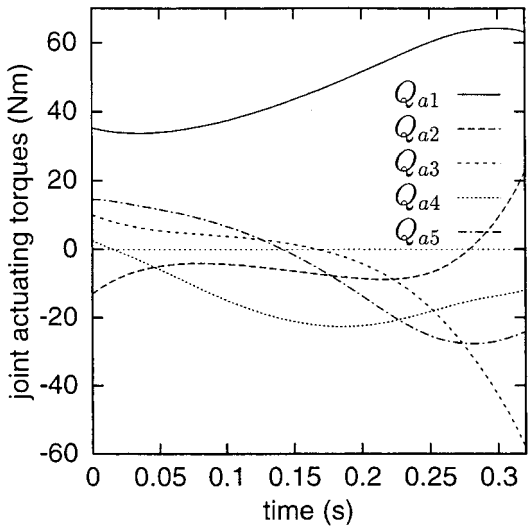

Fig. 20. Evolution of joint actuating torques.

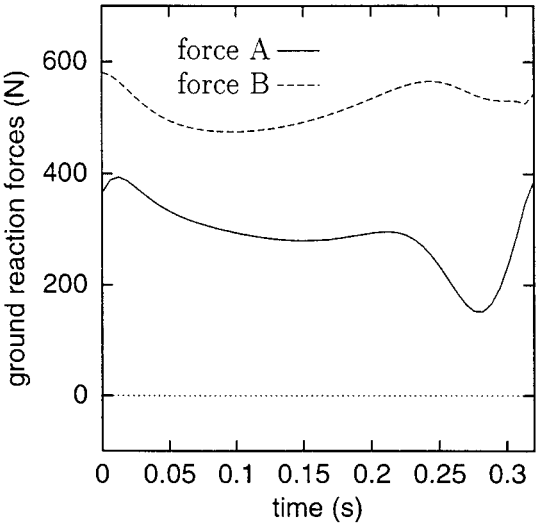

Fig. 21. Normal ground reaction forces.

generate a natural swing which is similar to the previous one from a kinematic standpoint. We emphasized the dynamic differences between these two motions, which raised the problem of their sensitivity to specified end conditions.

On this subject, an improvement of the approach presented would consist in specifying a minimum of initial and final constraints in order to deal with a less constrained problem. It would be possible as well to take into account the impact velocity at heel-touch. Pontryagin's maximum principle seems quite appropriate to deal with an extended problem of this type.

On the other hand, the double support phase remains to be dealt with. Since the biped performs as a closed kinematics chain during a brief lapse of time, a simple means to tackle this problem may consist in specifying the kinematics of motion that brings the end of the preceding unipodal phase to the beginning of the next one. This approach will result in solving an inverse dynamic problem. But, for the mechanical system having a closed kinematic loop, this problem is undetermined. However, it would be possible to extract a solution of minimal norm in terms of joint actuating torques and contact forces by using, for instance, a pseudo-inverse matrix technique as implemented in reference (29) to solve a cycling problem in the field of biomechanics. In another respect, the bipodal phase problem could as well be solved using the maximum principle.

To conclude, a final problem would consist in matching optimally both phases of gait in order to generate a global optimal step.

References

1. C.K. Chow & D.H. Jacobson, "Studies of Human Locomotion via optimal Programming," *Mathematical Biosciences* **10**, 239–306 (1971).
2. H. Hatze, "The complete optimization of a human motion," *Mathematical Biosciences* **28**, 99–135 (1976).
3. P. Bourassa, Y. Morel & B. Marcos, "Human locomotion via optimal programming," *Biomechanics* **5a(IX-A)**, 673–677 (1985).
4. J.V.V. Beletskii & P.S. Cludinov, "Parametric optimization in the problem of biped locomotion," *Izv. AN SSSR. Mekhanika Tverdogo Tela* **12**(1), 25–35 (1997).

https://doi.org/10.1017/S0263574700003039 Published online by Cambridge University Press

5. V. Yen & L. Nagurka, "Soboptimal trajectory planning of a five-link human locomotion model," **In:** *Biomechanics of Normal and Prosthetic Gait, ASME Winter Annual Meeting*, Boston (1987) pp. 17–22.
6. P.H. Channon, S.H. Hopkins & D.T. Pham, "Derivation of optimal walking motions for a bipedal walking robot," *Robotica* **10**, Part 2, 165–172 (1992).
7. C. Chevallereau & Y. Aoustin, "Optimal joint reference trajectories for generation of gait cycles for walking and running of a biped robot," *Rapport Interne No. 99.07* (IRCyN, Nantes, France, 1999).
8. G. Cabodevila & G. Abba, "Quasi optimal gait for a biped robot using genetic algorithm," *Proc. IEEE Int. Conf. on Systems, Man, and Cybernetics*, Orlando (Oct. 1997) pp. 3960–3965.
9. L. Roussel, "Génération de trajectoires de marche optimale pour un robot bipède," *Thesis* (I.N.P. of Grenoble, France, 1998).
10. R.N. Marshall, G.A. Wood & L.S. Jennings, "Performance objectives in human movement: a review and application to the stance phase of normal walking," *Human Movement Science* **8**, 571–594 (1989).
11. H. Miura & I. Shimoyama, "Dynamic Walk of a Biped," *Int. J. Robot. Res.* **3**, No. 2, 60–74 (1984).
12. W. Miller, "Real-Time Neural Network Control of a Biped Walking Robot," *IEEE Control Systems* **14**, 41–48 (Feb. 1994).
13. J. Pratt & G. Pratt, "Intuitive Control of a Planar Bipedal Walking Robot," *Proc. of the IEEE-ICRA*, Belgium (May, 1998) pp. 2014–2021.
14. J. Yamaguchi, S. Inoue & A. Takanishi, "Development of a Bipedal Humunoid Robot "WABIAN" – Control method of whole body cooperative dynamic biped walking compensating for three-axis moment by trunk motion," *Proc. of the 12th CISM-IFToMM Symposium, Romansy 12*, Paris (1998) pp. 377–384.
15. K. Hirai, M. Hirose, Y. Haikawa & T. Takenaka, "The Development of Honda Humanoid Robot," *Proc. of the IEEE-ICRA*, Leuven, Belgium (1998) pp. 1321–1326.
16. W. Blajer & W. Schiehlen, "Walking Without Impacts as a Motion/Force Control Problem," *ASME Journal of Dynamic Systems* **114**, 660–665 (December, 1992).
17. G. Bessonnet, "Optimisation dynamique des mouvements point à point de robots manipulateurs," *Thesis* (University of Poitiers, France, 1992).
18. A.D. Jutard-Malinge & G. Bessonnet, "Optimal path planning of manipulatory systems subjected to non-autonomous motion laws," *Robotica* **15**, Part 3, 251–261 (1997).
19. M. Rostami & G. Bessonnet, "Impactless sagittal gait of a biped robot during the single support phase," *Proceedings of the 1998 IEEE, International Conference on Robotics & Automation*, Leuven, Belgium, May, 1998, **Vol. 2**, pp. 1385–1391.
20. M. Rostami, G. Bessonnet & P. Sardin, "Optimal gait synthesis of a planar biped," *The 3rd IFAC International Workshop on Motion Control*, Grenoble, France (Sept, 1998) 185–190.
21. F. Danes, M. Rostami & G. Bessonnet, "Flexion-Extension Movements of an Anthropomorphic Biped Robot," *5th IASTED Int. Conf. on Robotics and Manufacturing*, Cancún, Mexico (May, 1997) pp. 32–36.
22. M. Rostami, "Contribution à l'étude dynamique de la phase de la marche sagittale, et étude du comportement dynamique d'un membre locomoteur anthropomorphe de robot bipède," *Thesis* (University of Poitiers, France, March 1999).
23. G. Bessonnet & F. Danes, "Optimal motion generation involving non-smooth performance criterions," *World Automation Congress, Robotic and Manufacturing Systems Anchorage* (1998) **Vol. 7**, pp. 79–86.
24. A.V. Fiacco & G.P. Cormick, "The slacked unconstrained minimization technique for convex programming," *J. Applied Mathematics*, **15**(3), 505–515 (1967).
25. F.L. Lewis & V.L. Syrmos, *Optimal Control* (John Wiley, 1995).
26. A.E. Bryson & Y.C. Ho, *Applied Optimal Control* (Hemisphere Publishing Corporation, 1969).
27. P. Sardain, M. Rostami & G. Bessonnet, "An Anthropomorphic Biped Robot: Dynamic Concepts and Technological Design," *IEEE Transactions on Systems Man and Cybernetics* **28**(6), 823–838 (Nov., 1998).
28. P. Sardain, M. Rostami, E. Thomas & G. Bessonnet, "Biped robots: Correlation between technological design and dynamic behavior," *Control Engineering Practice, Journal of IFAC* **7**, 401–411 (1999).
29. O. Coussi, "De l'observation cinématique à l'étude dynamique et énergétique de mouvements humains," *Thesis* (University of Poitiers, France, Sept., 1997).

Appendix
Dimensional characteristics of the biped "BIP".

Dimensions of links (see Figure 1):

$$O_j\vec{O}_{j+1} = r_j\vec{X}_j \ , \ j = 1, \ \ldots, \ 5$$

$$(r_1, r_2, r_3, r_4, r_5) = (0.4, 0.41, 0, 0.41, 0.4)(m)$$

Foot dimensions

$$(O_1A, O_1B, AB) = (0.12, 0.165, 0.2)(m)$$

Positions of the centers of gravity:

$$\vec{O_i G_i} = a_i\vec{X}_i + b_i\vec{Y}_i \ , \ i = 1, \ \ldots, \ 6$$

$$(a_1,a_2,a_3,a_4,a_5,a_6) = (0.24,0.27,0.33,0.14,0.163,0.004)(m)$$

$$(b_1,b_2,b_3,b_4,b_5,b_6) = (0,0,0,0,0,0.08)(m)$$

Link masses:

$$(m_1,m_2,m_3,m_4,m_5,m_6) = (6.4,8.6,55.0,8.6,6.4,1.1)(kg)$$

Moments of inertia of links L_i about O_i

$$(I_1^{zz}, \ I_2^{zz}, I_3^{zz}, I_4^{zz}, I_5^{zz}, I_6^{zz})$$
$$= (0.44, 0.69, 7.0, 0.23, 0.25, 0.015)(kg.m^2)$$

https://doi.org/10.1017/S0263574700003039 Published online by Cambridge University Press